

A Large-Scale Test Vehicle for VTOL Ground Effects Studies

W. W. WATSON,* RAHIM LAVI,† AND H. ASDURIAN‡
Northrop Corporation, Norair Division, Hawthorne, Calif.

A large-scale boiler plate VTOL test bed was designed and fabricated around the Ames Lift Engine Pod. Ground proximity tests were conducted in cooperation with Ames Research Center at the Ames VTOL test facility. Program objectives were to establish VTOL aircraft environmental characteristics during near-ground operation and to determine the degree of hot gas ingestion and induced lift effects experienced by a number of potential VTOL fighter configurations. The results showed, as expected, that both ingestion and induced lift effects are strongly configuration-dependent, and for some configurations the degree of ingestion experienced cannot be tolerated in an operational aircraft. Rapid inlet temperature rise with a high temperature distortion at the compressor face generally resulted in engine stall. For certain engine groupings, wing, and lift/cruise inlet locations, hot gas ingestion was greatly minimized. Results also showed that transient measurements with rapid-response thermocouple and recording equipment are needed for realistic assessment of the VTOL environment and for inlet temperature rise caused by ingestion.

Introduction

INGESTION of hot exhaust gases by the engine of jet-powered VTOL aircraft in ground proximity is a serious problem that must be considered in the design of an operational aircraft. In addition, jet-exhaust induced flow on the lower surfaces of the vehicle may create forces affecting lift capability and stability.

Since ground proximity effects are highly configuration-dependent, the results of small-scale tests employing a single or dual jet arrangement cannot be readily extended to full-scale configurations employing various arrangements of lift or lift-plus-lift/cruise engines. Also, the limited data from the small-scale tests have not been developed adequately to permit extension of model data to full-scale. Thus the need for realistic data on hot gas ingestion and jet effects became evident and led to design and testing of a large-scale captive jet-lift vehicle capable of representing a number of potential jet-lift VTOL configurations.

Large-scale tests of VTOL configurations employing various arrangements of lift or lift-plus-lift/cruise engines were conducted to determine: 1) inlet temperature rise due to hot gas ingestion for various potential jet-lift VTOL configurations, 2) the influence of hot gas ingestion on engine performance and operating characteristics, and 3) the jet-induced lift effects in ground proximity.

Design Philosophy

In early 1965 a decision was made by Northrop Norair to obtain realistic ground proximity effects data for various jet VTOL study configurations by employing a large-scale test vehicle equipped with lift-plus-lift/cruise engines. Studies showed that a number of potential jet lift VTOL configurations could be evolved from the modification of the existing

Ames lift engine pod. Thus, experimental investigation of a number of potential jet-lift configurations was economically feasible. NASA Ames Research Center granted permission for the use of the pod and a joint cooperative program to investigate ground proximity effects was initiated.

The Ames lift engine pod (Fig. 1) is a structural steel framework approximately 13 ft long, 2 ft wide, and 4 ft high, mounting five YJ85-GE-5 engines (without afterburners) on 30.5-in. centers. The engines are modified for vertical operation, with thrust lines tilted 10° aft from the vertical. Electric starters are installed, but power and fuel are supplied externally. In its original configuration, the pod also utilized short nose and aft fairings, and was supported in the wind tunnel or test stand from the tips of stub wings of a 16-ft span.

The test vehicle (Fig. 2) was designed to approximate the proportions of a representative composite supersonic fighter jet-lift vehicle. Major modifications to the lift engine pod to represent the desired potential configurations included the addition of an extended fore-body, and aft fuselage mounting two horizontal engines, wings and horizontal tail surfaces, exhaust ejectors, and exhaust vectoring doors.

A welded tube structure was attached to the back of the lift engine pod as the main framework for the aft fuselage section. Since only planform and lower surface representation were desired, the lower half of this structure was covered with thin metal skin, but the upper half was left open. In order to represent a composite arrangement of lift and lift/-cruise propulsion, two additional engines were mounted horizontally in this aft fuselage. These engines, simulating combination lift and cruise propulsion units, were equipped with right-angle tailpipes to permit downward exhaust flow. These

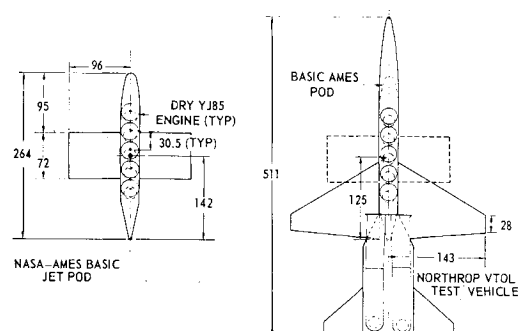


Fig. 1 Comparison of original and modified vehicles.

Presented as Paper 67-181 at the AIAA 5th Aerospace Sciences Meeting, New York, January 23-26, 1967; submitted March 30, 1967; revision received August 3, 1967. The authors wish to express their gratitude to the NASA-Ames Large-Scale Aerodynamics Branch for use of the lift engine pod and VTO Test Facility; and to W. H. Tolhurst Jr. for his valuable assistance and support throughout the test program. [3.01, 7.06, 7.11, 10.09]

* Engineering Specialist, Research Design Group. Member AIAA.

† Senior Scientist, Aerodynamics and Propulsion Research and Technology Group. Member AIAA.

‡ Member of Technical Management, Advanced Aircraft Systems Section. Member AIAA.

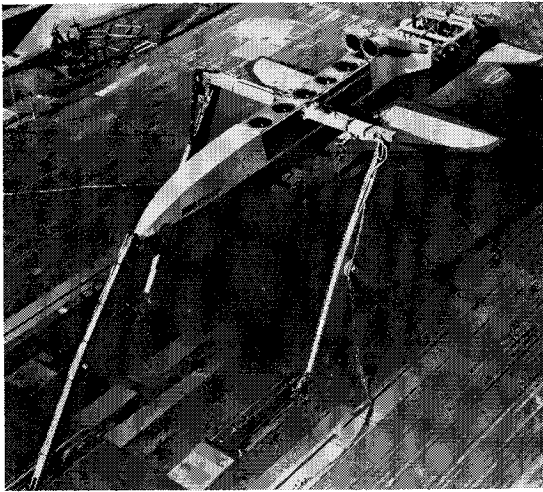


Fig. 2 Test vehicle mounted on NASA-Ames VTO stand.

engines were similar to the lift engines (J85) utilized in the pod.

A welded steel truss with skin surface formed the nose fairing, and served as the nose support member in the three-point vehicle mount system of the Ames static test stand. A fixed structural beam 16 ft long was mounted through the fuselage between inlets of engines 2 and 3 as the main support, allowing the wings to be bolted directly to the side of the vehicle. From a previous test, T-38 wings and horizontal tail surfaces were made available. The wing roots were bolted by attachment plates to the sides of the engine pod, and the tail was mounted by its torque tube. Additional wing planforms were fabricated and were evaluated in a subsequent test program.¹

Rapid-response electric throttle actuators and adjustable limit switches were used to permit burst acceleration of the engine from the selected idle condition to 100% rpm in approximately one sec. Hydraulically actuated exhaust vectoring doors installed for each engine were capable of vectoring the engine exhaust forward to produce a straight down flow and aft 60°. Adjustable stops on the actuation cylinders at each end of the travel permitted vector control within this range. The vectoring door geometry, selected from small-scale tests of various configurations, was effective in turning the exhaust flow as much as 60° without adversely affecting engine operation. Ejectors were installed on the lift-engine

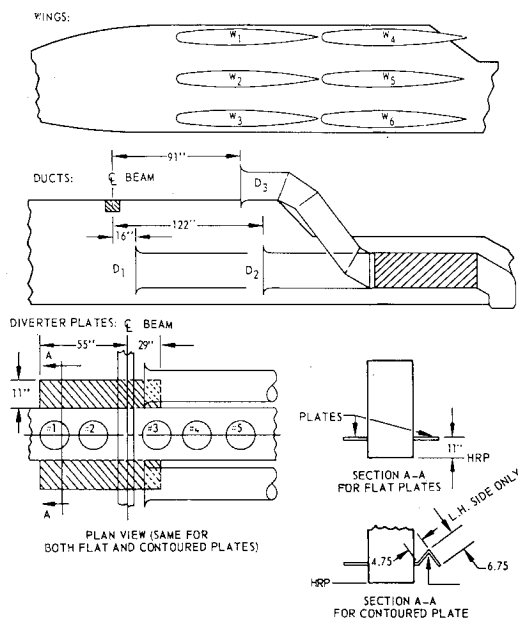


Fig. 3 Configuration variables.

exhausts to provide airflow for adequate cooling of the engine bays.

The lift/cruise engines were fitted with alternate ducting to allow three inlet locations: along the fuselage sides near the wing trailing edge, along the fuselage sides just ahead of the wing leading edge, and above the fuselage side-by-side just aft of the number 5 lift engine inlet. Six wing locations were possible: high, medium or low position, either relatively forward or aft (37-in. lateral variation). In addition, any combination of lift and lift-plus-lift/cruise engines could be run to represent various engine groupings. Figure 3 shows the configuration variables.

Instrumentation

Test instrumentation fell into the following groups.

1) Vehicle force and moments: The model was mounted on three biaxial load cells, one at each tip of the main support beam, and one at the nose support point (Fig.4). The main beam load cells were connected to record both normal and axial force measurements, and the nose beam cell, normal only. This was possible because the upper end of the support stand nose beam was connected to the load cell through a toggle arm, to allow the vehicle to be pitched. The toggle also served, however, to transmit only vertical loads (plus small horizontal loads resulting from its inclination from the vertical) to the load cell. These horizontal interaction loads were accounted for in the data reduction equations. The five force data channels were recorded on a CEC oscillograph and reduced to three components: normal force, axial force, and pitching moment. The vehicle/load cell system was calibrated to 8,000-lb total axial force, 16,000-lb total normal force, and 1,000,000 lb-in. pitching moment. All first-order interactions were considered in the equations.

2) Engine performance parameters: Exhaust nozzle total pressure and temperature of each engine were recorded continuously on oscillographs during each test. Indications of engine speed and exhaust gas temperature for all engines were provided in the engine-control console and monitored by the operators during each test. In addition, engine rpm of one lift engine and one lift/cruise engine were continuously recorded.

3) Engine inlet temperatures: Eight iron-constantan (30 gage) 0.01-in.-diam. thermocouples were installed in the inlets of all engines. The installation consisted of two rakes with three thermocouples each, located on the forward and left side radii, and single thermocouples near the outer wall on the aft and right side, respectively. The rake thermocouples were spaced to define inlet temperatures over approximately equal flow areas.

A high-temperature (150°F) reference system was used and the outputs of the thermocouples were continuously re-

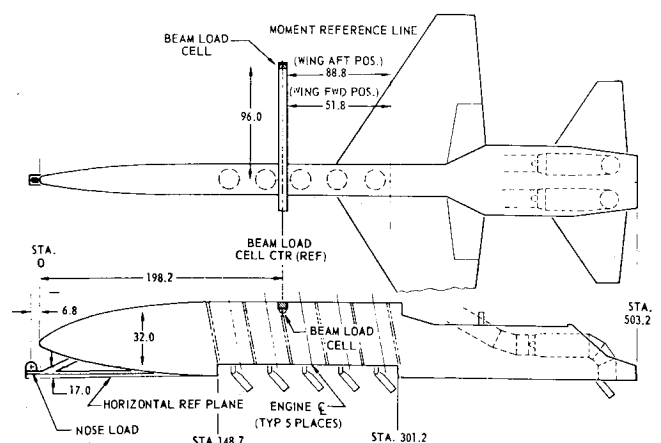


Fig. 4 Load cell locations.

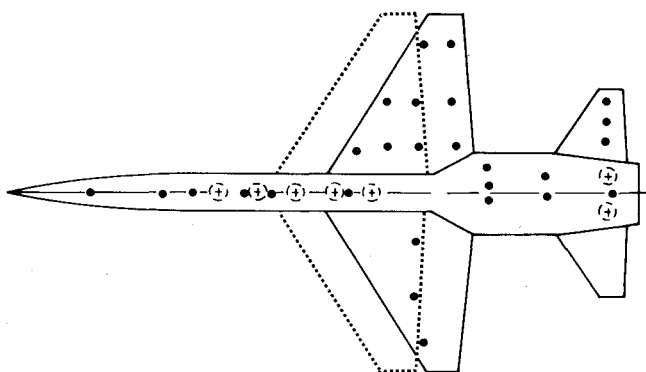


Fig. 5 Vehicle static pressure taps.

corded by color traces on oscillographs to obtain the fast response and distinction of traces necessary to show rapid temperature variations. The time constant for the thermocouple-recording system combination was determined to be of the order of 120 msec. Immediately following a compressor stall, a burst of hot gas is discharged back through the compressor, resulting in an approximate step-input temperature change at the inlet thermocouples. An analysis of the oscillographic traces during several compressor stalls indicated an over-all response rate capability of the order of $2000^{\circ}\text{F}/\text{sec}$.

4) Vehicle pressures: Static pressure taps were located on the underside of the fuselage, wings and horizontal tail (Fig. 5). These pressures were measured on a water manometer board, and were recorded photographically. In addition, transient static pressure measurements from transducers at four locations on the wing lower surface were oscillographically recorded.

5) Ground plane pressure and temperatures: Five static pressure probes mounted 1 in. off the ground plane, and four in a rake, from 1 to 18 in. high were read on a water manometer (Fig. 6). These probes could be moved to various locations to map the ground plane pressure environment.

Two I/C thermocouples, calibrated up to 550°F and seven C/A thermocouples calibrated to 1400°F , were installed on plates mounted on the ground plane. Like the ground plane pressure survey tubes, these could be relocated between runs to survey the area.

6) Vehicle temperatures: Thermocouples were installed in selected locations to monitor temperatures in the hydraulic system, on heat-sensitive electrical equipment, engine accessories and vehicle structure.

7) Acoustic environment: Ten channels were recorded: seven from microphones mounted on the side and underside

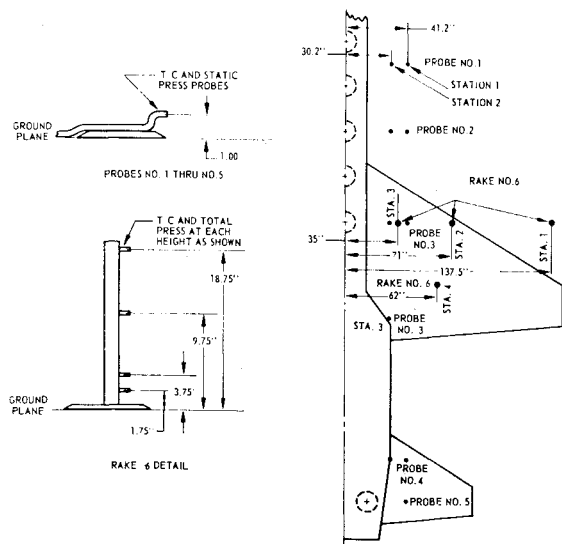


Fig. 6 Ground plane temperature and pressure probes.

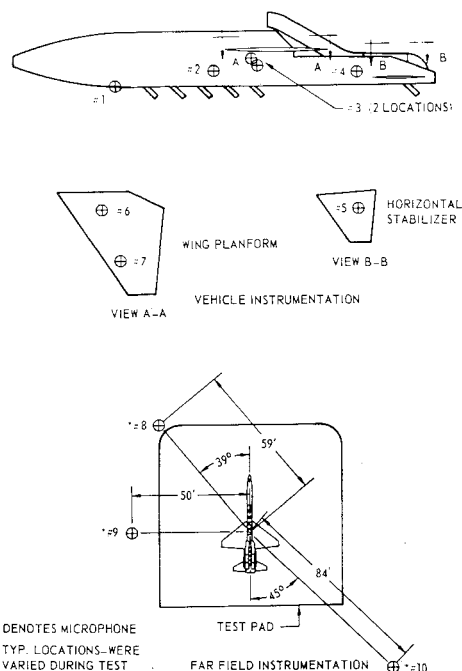


Fig. 7 Acoustic instrumentation location.

of the vehicle (Bruel & Kjaer no. 4136) and three on movable stands on the ground plane (B&K no. 4134). The vehicle microphones were calibrated on 180 db, 50 Hz-10 kHz, and the ground plane units to 160 db, 50 Hz-10 kHz. The height of the ground plane microphone stands could be varied and the microphones moved to different locations to survey the field. The location of the acoustic instrumentation is shown in Fig. 7.

8) Ambient instrumentation: Before each run, readings of ambient temperature, barometric pressure, and wind velocity and direction were hand recorded.

Test Facility

The Ames Research Center Static Test Facility is an outdoor test complex designed to support a wide range of powered models and aircraft at varying ground heights and angles of

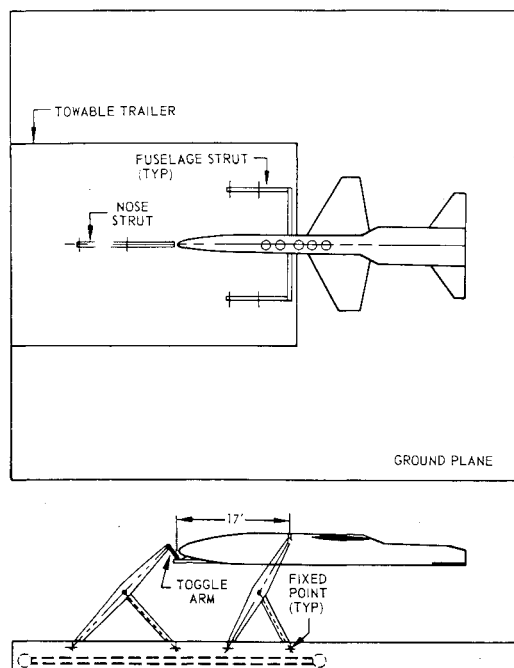



Fig. 8 Ames VTO thrust stand general arrangement.



CRUISE ENGINE INLET CONFIGURATION	LIFT ENGINE CONFIGURATION #1 (FRONT 4 ENGINES - WING AFT)			LIFT ENGINE CONFIGURATION #2 (FIRST 3 ENG PLUS AFT ENG - WING FWD)			LIFT ENGINE CONFIGURATION #3 (AFT 3 ENGINES - WING FWD)	
	LOW WING	MID WING	HIGH WING	HIGH WING	MID WING	LOW WING	LOW WING	HIGH WING
TOP INLET	① ②	①	① ②	① ②	①	① ③		
REAR INLET	①		①	①		① ②		
FORWARD INLET	① ③		①	①		① ②		
CRUISE ENGINE INOPERATIVE (TOP INLET)	①		①	①		①	①	①
WING OFF (TOP INLET)		①			①			①

Fig. 9 Basic configuration evaluations. Notes: H/D schedules: ① H/D = 8.7, 6.5, 4.5, 3, and 2.4 @ $\theta = 0^\circ$; ② H/D = 3 and 2.4 @ $\theta = -3^\circ$, $+3^\circ$, and $+4.5^\circ$; ③ H/D = 8.7, 6.5, 4.5, 3, and 2.4 @ $\theta = -3^\circ$, $+3^\circ$, and -4.5° (θ = vehicle pitch attitude, degrees). Crossed out configurations not run.

attack. The system is comprised of a towable trailer containing the motorized model support struts, a fixed ground plane test-site, and an office-type instrumentation trailer.

The support trailer and ground plane formed a flat 78 × 80-ft ground plane. The test vehicle was mounted on the thrust stand by three beams, one extending from each side of the fuselage just forward of the wing, another extending below the nose (to take out pitch loads via a toggle mechanism). This mounting is shown schematically in Fig. 8. The mounting arrangement was specifically selected to minimize flow interference by the support struts; this arrangement resulted in the engines exhausting aft of the primary mounting struts. Two-axis load cells were located on each side of the main support beam, and the third was attached through the load cell at the nose. All power to, and instrumentation from, the vehicle was routed under the ground plane and along the top of one of these support arms. Vehicle height variation from approximately 2.5 to 10 ft and pitch attitudes of -3° to $+4.5^\circ$ could be achieved for this particular test vehicle.

A small office trailer located approximately 50 ft from the stand served as a control room containing all data-recording equipment and the two engine run consoles, one controlling the five lift engines, the other the two lift/cruise engines. All engine instrumentation (rpm, exhaust gas temperature, throttle position indicator, etc.) as well as throttle actuator control switches, and controls for starter, ignition, deflector doors, and hydraulics were installed in this trailer. Electrical and hydraulic power, cooling water, fuel, and compressed air were supplied to the test stand.

Test Procedure

The normal test procedure was to stabilize all test engines at 70% rpm with the exhausts vectored rearward by the exhaust vectoring doors to preclude gas ingestion. An effective vectoring angle of 50° from vertical was selected as representative of an operational concept. On signal, the vectoring doors were rotated downward simultaneously with the application of military power on all test engines. Military power was held for intervals varying from approximately 5 sec at low vehicle heights to 20 sec at the highest height. These time periods were selected to represent at least twice the exposure time associated with an upward vehicle acceleration of 0.02 g. The initial engine speed of 70% rpm, which is higher than normal idle for the J85 engine, was selected to provide a rapid burst

acceleration to military power. The rotation of the vectoring doors and acceleration to military power were accomplished in about one sec. Data acquisition of transient parameters was initiated when the engines were at 70% rpm, and continued to the end of the run.

With minor exceptions, each configuration was tested at five heights. In terms of height-to-exhaust diameter ratios (H/D), the heights tested were 2.4, 3.0, 4.5, 6.5, and 8.7. Actual test heights ranged from 2.75 to a maximum of 10 ft, as measured from the bottom surface of the vehicle to the ground plane. Selected configurations were also tested with pitch attitudes varying from $+4.5^\circ$ to -3.0° at each height. A summary of the configurations evaluated is shown in Fig. 9. In addition, special tests were conducted to investigate gas ingestion with some degree of vectoring (10° and 20° aft) during full-power operation and during simulated start-ups with no vectoring (vertical exhaust). The latter tests were conducted to simulate start-up of vertically mounted engine not equipped with exhaust vectoring provisions.

Results

The thermocouple and recording equipment employed in this test program provided a realistic measurement of the transient nature of the hot exhaust gases ingested by the engines. It was found that the inlet temperature rise resulting from hot gas ingestion was, in general, strongly time-dependent and sporadic.

Figure 10a-e shows typical engine inlet time histories for an ingestion-prone configuration employing an arrangement of three lift engines forward and one aft of the wing box, with two lift/cruise engines in the tail. The wing was in the high forward position, and the lift/cruise engine inlets in the front positions. The data are for H/D = 3.0, where maximum ingestion was experienced. This configuration produced considerably more ingestion than most, but the data are presented to show the degree of ingestion that may result for an ingestion-prone configuration.

A high degree of ingestion with large temperature distortion was experienced by lift engines 1, 2, and 3. Rapid inlet temperature rise and/or highly distorted inlet temperature profile can cause engine stall. Both phenomena were observed in the inlet of number 1 engine and resulted in engine stall 3.9 sec after the engine reached 100% rpm. The large, rapid temperature rise subsequent to engine stall is caused by the

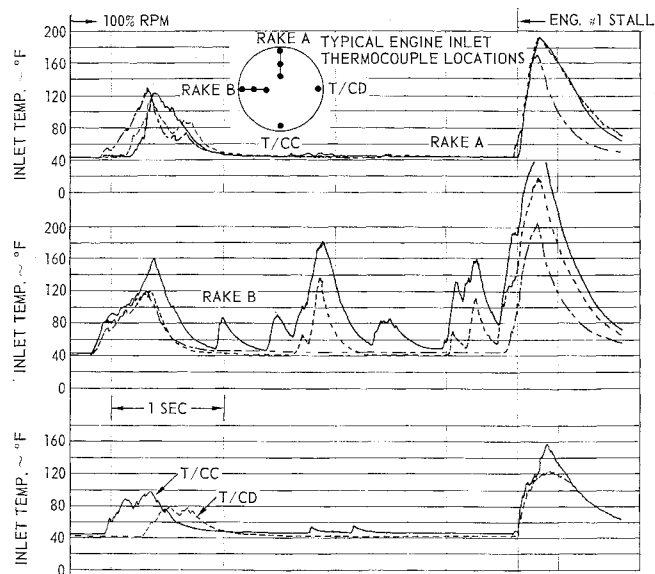


Fig. 10a Lift engine no. 1.

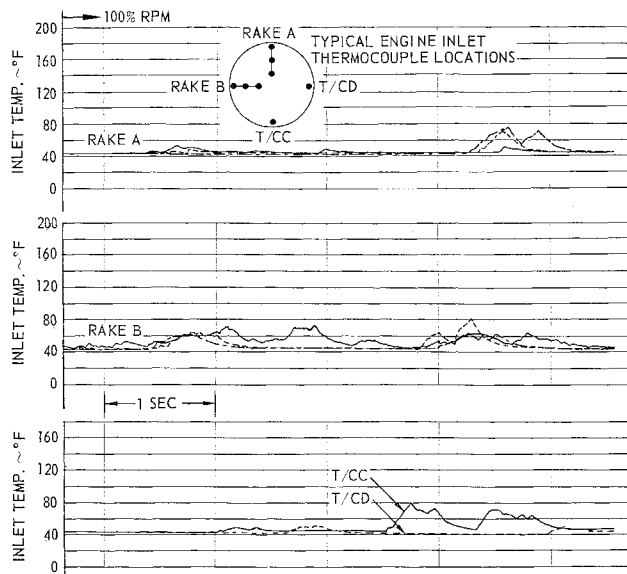


Fig. 10d Lift engine no. 5.

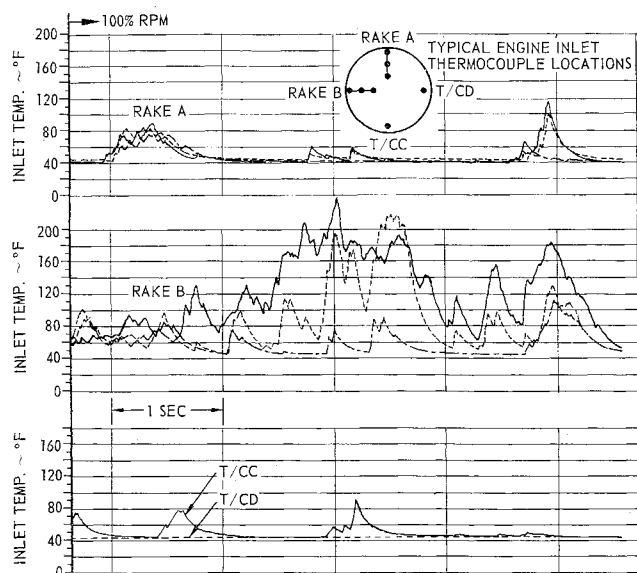


Fig. 10b Lift engine no. 2.

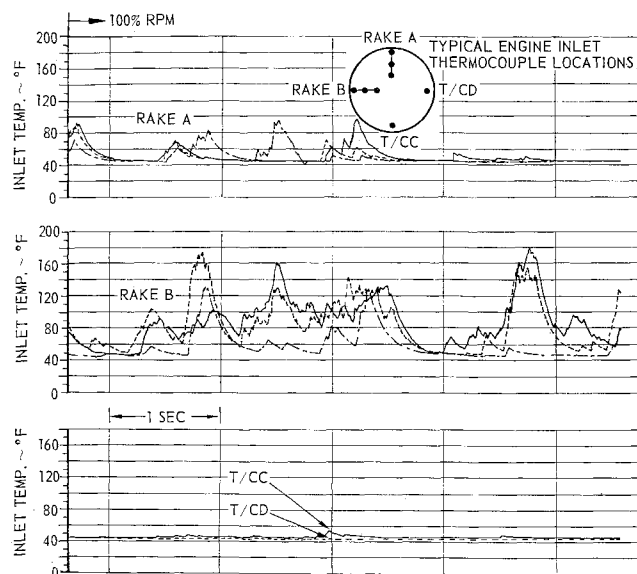


Fig. 10c Lift engine no. 3.

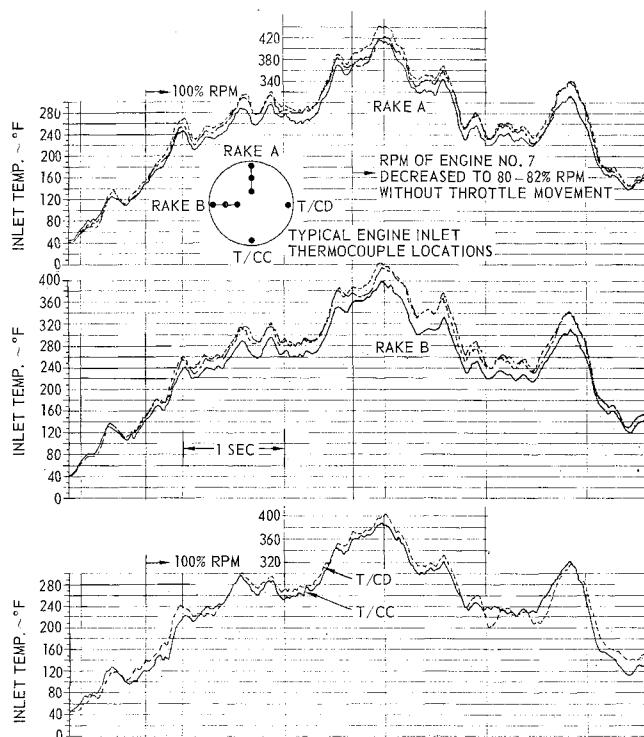


Fig. 10e L. H. lift/cruise engine (no. 7).

back flow of hot internal gases expelled from the engine. These gases from one lift engine may stall adjacent engines, although this did not occur in the particular run under consideration.

The lift/cruise engines in general exhibited a more uniform temperature rise (low distortion) compared to the lift engines as shown in Fig. 10e. The long duct leading to the lift/cruise engines allowed sufficient time for mixing of the hot gases, and thus resulted in a relatively uniform temperature field at the compressor face. As a result, lift/cruise engine stall was an infrequent occurrence.

The wing location had a pronounced influence on the degree of ingested hot gas. For instance, the propulsion system arrangement discussed previously was evaluated with a low and aft wing location. For this configuration, the ingestion was considerably reduced, because the wing deflected the high velocity hot gases away from the inlets. A sketch of the

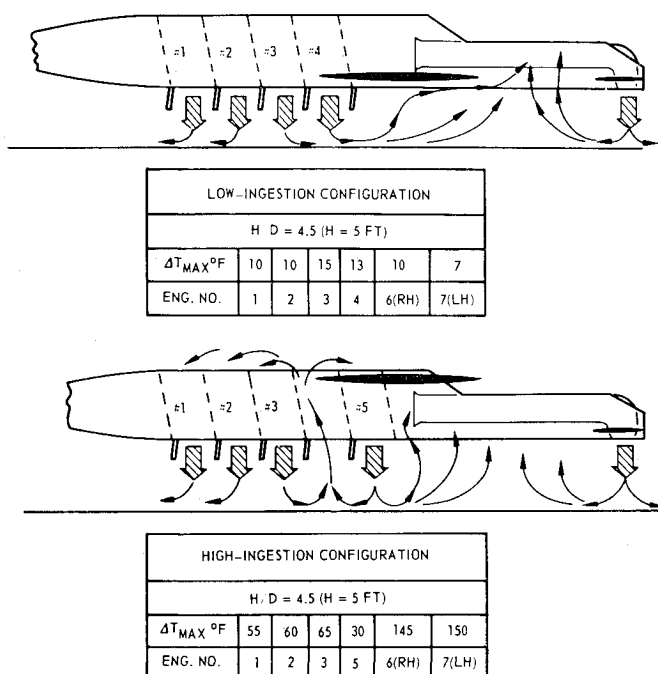


Fig. 11 Effect of configuration on gas ingestion.

flowfield and the effect of the wing location is shown in Fig. 11.

Jet-induced lift effects resulted in positive or negative lift forces depending on wing locations, engine arrangement, and height above ground. In general, negative induced lift was between 4 to 6% in free air. A typical variation of induced lift with height above ground and wing position is shown in Fig. 12.

Special Tests

Acoustic Field

The objective of the acoustic portion of the test was to develop a method of approximating the maximum sound pressure levels on the exposed surfaces of the vehicle and in the area surrounding a comparable VTOL aircraft configuration. Sound pressure levels from 148 to 156 db were recorded by the seven microphones installed at various locations on the test vehicle. It was found that sound levels were significantly less at H/D of 2.4 as compared to higher vehicle heights above ground. At a distance of 50–85 ft from the vehicle, noise levels increased with vehicle height above ground and were of the order of 130 db at a height of 8.7-exhaust diam above the ground.

Wheel and Tire Temperatures

An aircraft wheel and tire were located at the nominal gear-down location to determine temperatures to which a wheel and tire of a typical fighter VTOL design would be subjected during a representative engine start up, idle, and lift-off opera-

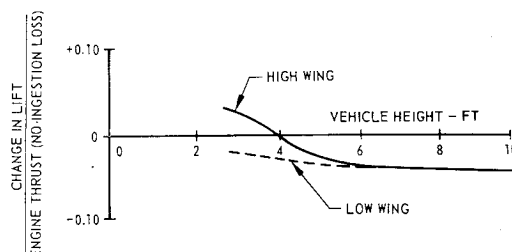


Fig. 12 Effect of wing position on jet-induced lift.

tion. Temperature indicating paint selected to indicate temperatures ranging from 150° to 350°F in approximate 25°F increments was applied to fourteen selected small areas of the wheel and tire. The test was conducted at the nominal landing gear height (H/D = 3.0) with composite engine configuration. Maximum temperature observed was 300°F.

Fence Tests

Limited tests of methods to reduce or preclude engine hot gas ingestion were conducted. These included longitudinal flat plates of approximately 0.7 inlet diam wide attached to the side of the fuselage. These fences formed an extension of the wing leading edge and were used during both high and low wing tests. The fences, in general, reduced ingestion but did not effectively eliminate the problem. Similar wing geometry but with a greater root chord would have been probably more effective than the fences evaluated here. Additional testing would be required to explore the full potential of physical shields.

Conclusions

- 1) The flowfield in the vicinity of the engine inlets developed by the combined effects of engine exhausts and intake airflows at low heights was highly unstable with intermittent hot and cold zones. The severity of the flowfield and the resulting hot gas ingested by the engines were highly dependent on the arrangement of the lift engines, wing position, and the location of the lift/cruise engine inlets.
- 2) Fast-response sensing and recording equipment are required to realistically assess the VTOL ground proximity environment.
- 3) Hot gas ingestion is a major potential problem for jet lift VTOL aircraft and must be considered during preliminary configuration design.
- 4) Jet-induced lift effects are of sufficient magnitude to be considered from the standpoint of required thrust and induced moment imbalance. However, hot gas ingestion could be an overriding consideration.

References

- 1 Lavi, R., "Parametric investigation of VTOL ground proximity effects," AIAA Paper 67-440 (July 1967).
- 2 Stark, W., et al. "Results of a hot gas ingestion and jet effects test program with a large scale VTOL test vehicle in ground proximity," Northrop Rept. NOR 66-246 (November 1966).